Materials Transactions, Vol. 47, No. 12 (2006) pp. 2898 to 2903

Dielectric Properties of Poly- and Single-Crystalline $BaTi_2O_5$

Rong Tu and Takashi Goto

Institute for Materials Research, Tohoku University, Sendai, Japan 980-8577

Non-oriented and (010) oriented poly-crystalline $BaTi_2O_5$ (BT_2) was prepared by hot-pressing and arc-melting, respectively. The dielectric properties of poly-crystalline BT_2 were compared with those of single-crystalline BT_2 prepared by a floating zone method. The maximum permittivity of (010) oriented poly-crystalline BT_2 was 2000 at 720 K, whereas that of single-crystalline BT_2 was 6000 at the Curie temperature, T_c (750 K). The permittivity of non-oriented poly-crystalline BT_2 was 30 to 300, having a small peak at 720 K. The $\tan\delta$ of all specimens was 0.01 to 0.2 below T_c and significantly increased with increasing temperature above T_c. The electrical conductivity of (010) oriented poly- and single-crystalline BT_2 had almost same values, which were one order higher than that of non-oriented poly-crystalline BT_2 and (001) oriented single-crystalline BT_2. [doi:10.2320/matertrans.47.2898]

(Received May 31, 2006; Accepted October 13, 2006; Published December 15, 2006)

Keywords: *$BaTi_2O_5$, poly-crystalline, single-crystalline, arc-melting, hot-pressing, floating zone method, permittivity, Curie temperature*

1. Introduction

Although the phase diagram of BaO-TiO_2 system has been studied for a long time, the ferroelectricity of $BaTi_2O_5$ (BT_2) has not been known until recently.[1–5] Our group[6,7] and Akishige *et al.*[8] independently synthesized single-crystalline BT_2 and reported the significant ferroelectricity only in the *b*-direction. Since BT_2 can be easily decomposed into $BaTiO_3$ (BT) and $Ba_6Ti_{17}O_{40}$ (B_6T_{17}) above 1500 K, large-scale crystalline BT_2 can be hardly prepared. In order to apply BT_2 for practical applications, the process to prepare *b*-axis oriented poly-crystalline BT_2 should be developed. Although the conventional solid state sintering process may not be applicable due to the decomposition of BT_2, Beltrán *et al.* have reported the preparation of non-oriented poly-crystalline BT_2 in a single phase by a sol-gel method, in which the T_c was about 750 K with the permittivity of 130.[9] It is known that needle-like single-crystalline BT_2 would precipitate from melts, where the growth direction is parallel to *b*-axis.[8] This suggests that the *b*-axis oriented poly-crystalline BT_2 can be prepared by a melt-solidification process. In the present study, an arc-melting method was applied to prepare the *b*-axis oriented poly-crystalline BT_2, and the dielectric properties were compared with those of non-oriented poly- and single-crystalline BT_2.

2. Experimental

Dried $BaCO_3$ and TiO_2 powders (purity: 99.9%) were weighed and mixed at the molar ratio of 1 to 2, and pressed into pellets (20 mm in dia., 5 mm in thick). The pellets were calcined at 1173 K in air for 43 ks and then melted with an arc using a tungsten electrode. The arc-melting apparatus was evacuated to 10^{-3} Pa and Ar gas was introduced into the chamber at 2.5 kPa. Button specimens were obtained by melting the pellets, which were quenched on a water-cooled copper plate, and were cut to coupons ($5 \times 5 \times 1$ mm) whose surface is parallel to the copper plate. The coupons were heat-treated at 1223 K for 43 ks in air. The button specimens were also crushed into powder. The powder was hot-pressed at 1473 K under 30 MPa for 43 ks in O_2 in an alumina die, and sintered bodies (10 mm in dia, 1 mm in thick) were obtained. A floating zone (FZ) method was used to prepare single-crystalline BT_2 whose surface were cut parallel to (001) and (010) planes[6] in size of $2 \times 2 \times 0.3$ mm. The crystal phase was identified by X-ray diffraction (XRD). The microstructure was observed by scanning electron microscope (SEM) after etching in an HCl + 10 vol% HF solution at room temperature. The composition was analyzed by electron probe microanalysis (EPMA). A gold paste was used as electrodes. The dielectric properties were measured in air with an impedance analysis (Hewlett Packard 4194) from 293 to 1073 K in a frequency (f) range between 10^2 and 10^7 Hz. The DC electrical conductivity was measured with a 2-probe method in air.

3. Results and Discussion

Figure 1 shows the XRD patterns of poly- and single-crystalline BT_2. The poly-crystalline BT_2 prepared by hot-pressing was in a single phase with almost no preferred orientation (Fig. 1(a), abbreviated as HP). The arc-melted poly-crystalline BT_2 (Fig. 1(b) as AR) had the significant (010) orientation. The single-crystalline BT_2 specimens

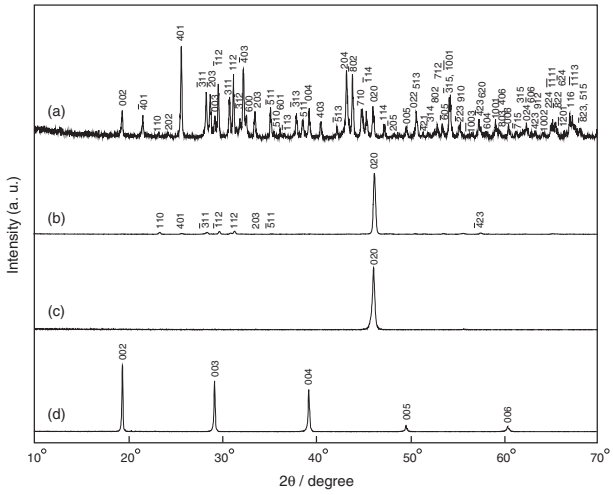

Fig. 1 X-ray diffraction patterns of poly- and single-crystalline BT_2 (a) HP, (b) AR, (c) *b*-FZ and (d) *c*-FZ.

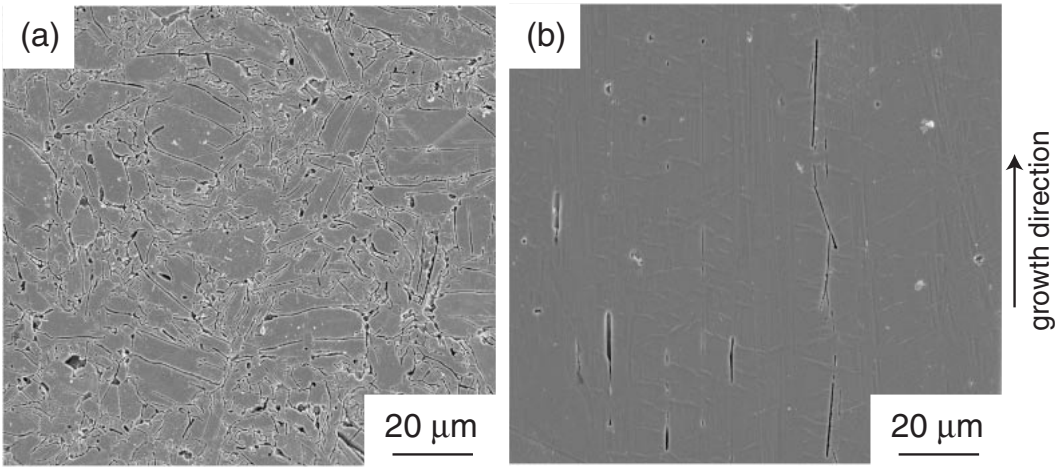

Fig. 2 SEM images of cross-section for poly-crystalline BT_2. (a) HP and (b) AR paralleled to growth direction.

whose (010) and (001) planes were parallel to the surface are abbreviated as *b*-FZ and *c*-FZ in Fig. 1, respectively.

Figure 2 depicts the SEM images of cross-section for HP and AR specimens parallel to the growth direction. Elongated grains were observed in the HP specimens (Fig. 2(a)). It is well known that BT_2 crystal may easily grow along the *b*-direction from the melt and needle-like BT_2 crystals were often prepared.[8,10] Although no report on the abnormal grain growth during the sintering of BT_2, the elongated direction might be the *b*-axis of BT_2. Many gaps at the grain boundaries might be formed by significant difference of the linear thermal expansion (α) among *a*-, *b*- and *c*-directions of BT_2 ($\alpha_a = 5.14$, $\alpha_b = 0.86$ and $\alpha_c = 12.5 \times 10^{-6}\,K^{-1}$ at 900 K[10]). The AR specimens were dense having a columnar texture along the growth direction (Fig. 2(b)). Since XRD data (Fig. 1(b)) showed significant (010) orientation, the growth direction of the columnar grains should be ⟨010⟩. As-melted AR specimens were dark blue which changed to white in color after heat-treatment in air, suggesting the compensation of oxide vacancy in the as-melted AR specimens. Since *b*-FZ and *c*-FZ specimens were dense with no specific feature, no SEM images were presented.

Figure 3 demonstrates the complex impedance plots at 743 and 973 K. At 743 K, the impedance of all specimens was too high to draw full semicircles at the present frequency range. The magnified view close to the original point was inserted in Fig. 3(a). The impedance of AR specimens was almost the same as that of *b*-FZ because both specimens were highly *b*-axis oriented. The HP specimen had intermediate value between *b*-FZ and *c*-FZ specimens consisting with the non-orientation. At 973 K, all specimens showed full semicircles crossing the original point. The capacitance values associated to the semicircle can be calculated at the top of semicircle from the relationship of $\omega\tau = 1$, where ω ($= 2\pi f$) is an angular frequency and τ ($= RC$, R: resistivity, C: capacitance) is a relaxation time. The associated capacitance values were 30, 60, 40 and 7 pF for AR, HP, *b*-FZ and *c*-FZ specimens, respectively. These values could be caused of the bulk response, and no grain boundary response was identified in the poly-crystalline AR and HP specimens suggesting no specific grain boundary phase.[11]

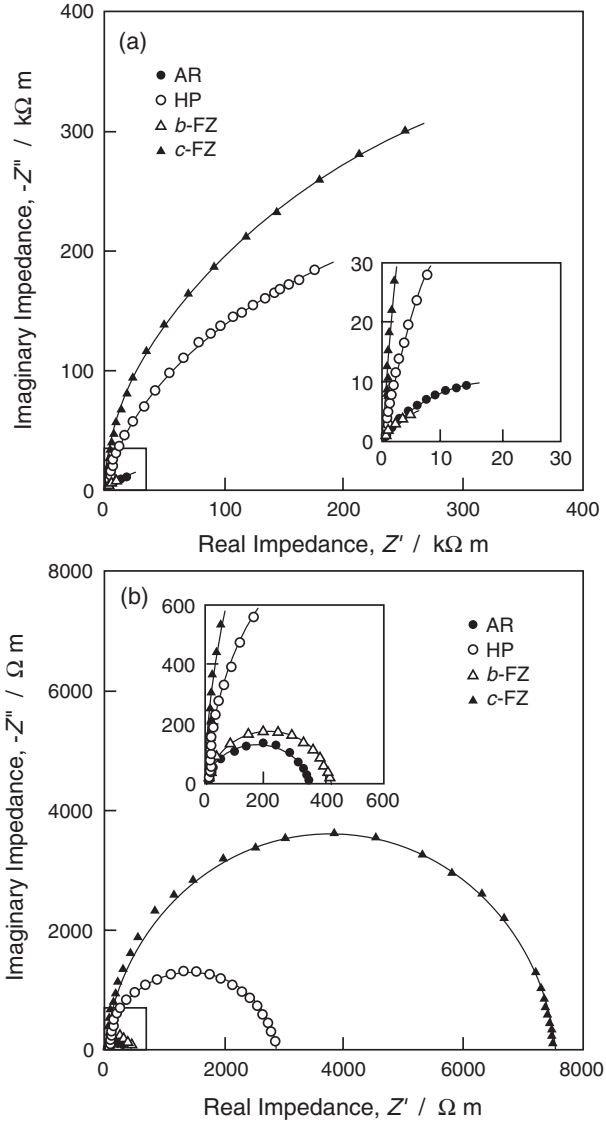

Fig. 3 Complex impedance plots at T = (a) 743 and (b) 973 K.

Figure 4 demonstrates the effect of frequency on the imaginary part of complex impedance (Z'') and modulus (M'') at 1023 K. The Z'' and M'' of all specimens showed a

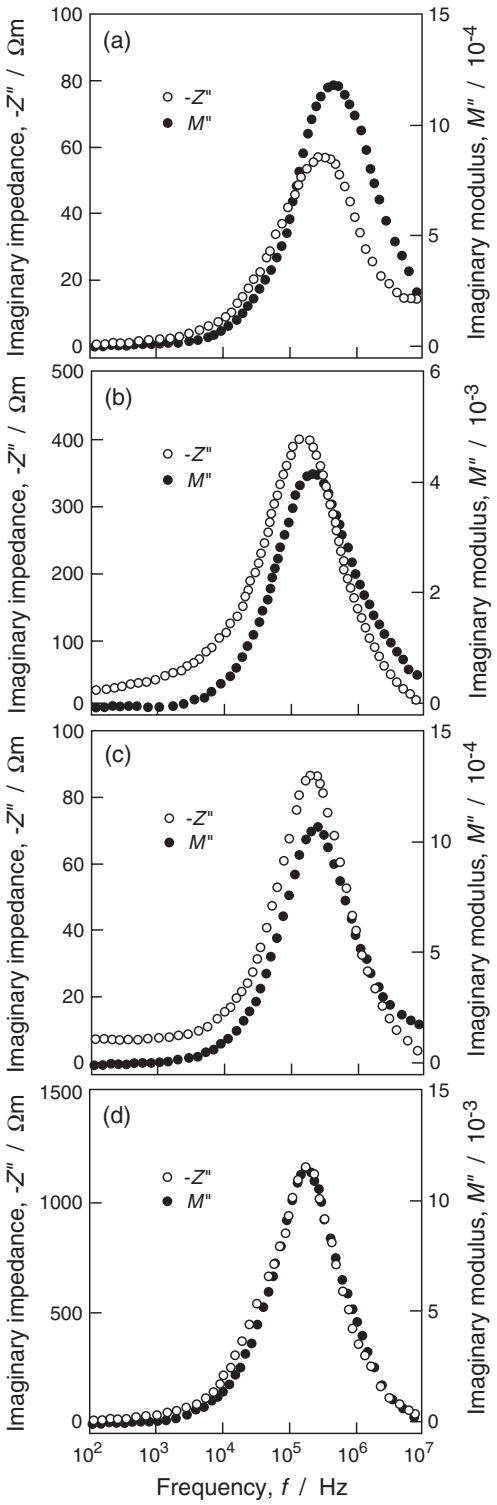

Fig. 4 Effect of frequency on imaginary impedance and modulus at 1023 K. (a) AR, (b) HP, (c) *b*-FZ and (d) *c*-FZ.

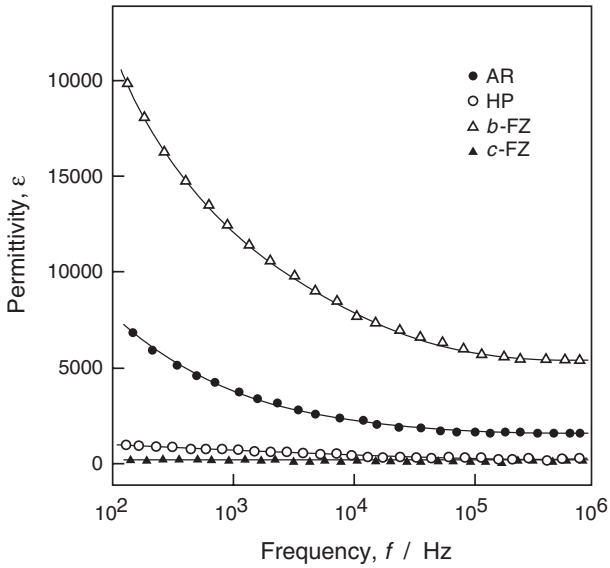

Fig. 5 Relationship between permittivity of and frequency at $T = 743$ K.

single peak, implying the bulk response. Beltrán *et al.* synthesized BT_2 powder by a sol-gel method, and sintered the BT_2 powder at 1373 K. They reported a single peak in Z'' and M'' vs. f relationships, implying the single bulk response.[9] No relaxation process from grain boundary or surface was reported, which is in agreement with that of present study. The peak frequency for Z'' ($f_{Z''}$) should be theoretically coincident with that for M'' ($f_{M''}$).[12] However, the $f_{Z''}$ often differs from the $f_{M''}$ resulting from the defect structure or imhomogeneity of specimens. Beltrán *et al.* reported the significant deference between $f_{Z''}$ and $f_{M''}$ at high temperatures due to the partial decomposition of BT_2.[9] On the other hand, the $f_{Z''}$ was almost in agreement to $f_{M''}$ in this study, suggesting homogeneous microstructure and no decomposition in the present BT_2 specimens. In the *c*-FZ specimen, the $f_{Z''}$ exactly agreed with the $f_{M''}$ implying a sharp distribution of relaxation time associating with high crystallinity and excellent *c*-orientation. The $f_{Z''}$ of AR and *b*-FZ specimens slightly shifted from the $f_{M''}$, suggesting a slight disordering of crystal orientation. The difference between $f_{Z''}$ and $f_{M''}$ for the HP specimen was smaller than that of poly-crystalline BT_2 sintered at 1473 by Beltrán *et al.*[9] This suggests that the HP specimen prepared by the powder from arc-melted buttons had higher thermal stability than that prepared by the sol-gel method.

Figure 5 depicts the frequency dependence of permittivity (ε) at 743 K. The permittivity decreased with increasing frequency and became almost constant over 100 kHz. Since the apparent permittivity would decrease with increasing frequency due to the resistivity component (R),[13] the true permittivity should be evaluated at a high frequency. Fig. 5 implies that the true permittivity can be obtained over 100 kHz. If the complex impedance plot had a full semicircle, the true permittivity can be obtained from the relationship of $\omega\tau = 1$ at the top of semicircle.[14] If the resistivity is too high to obtain the full semicircle of the complex impedance plot, the true permittivity can be obtained from the frequency dependence of permittivity at the high frequency.

Figure 6 demonstrates the temperature dependence of permittivity for all specimens at 100 kHz. All specimens showed peaks around 750 K implying the ferroelectric to paraelectric transition. Although the *b*-axis orientation of AR specimen was primarily similar to that of *b*-FZ specimen, the maximum permittivity of AR specimen was about 2000 which was smaller than that of *b*-FZ (~6000). The smaller permittivity of AR specimens could be associated with the

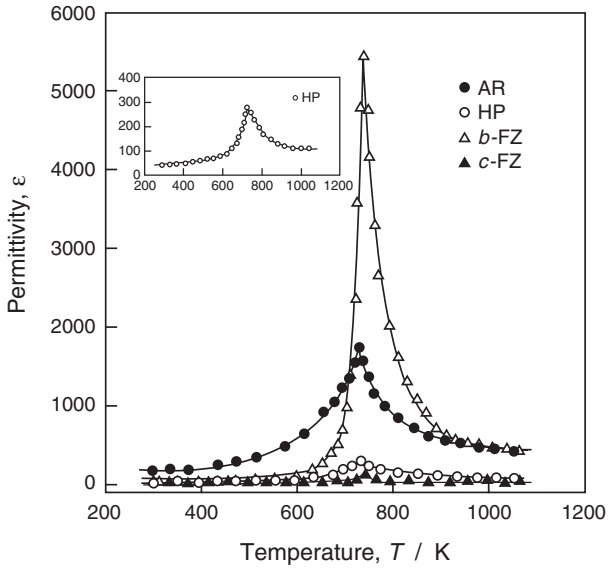

Fig. 6 Temperature dependence of permittivity for poly- and single-crystalline BT_2 at 100 kHz.

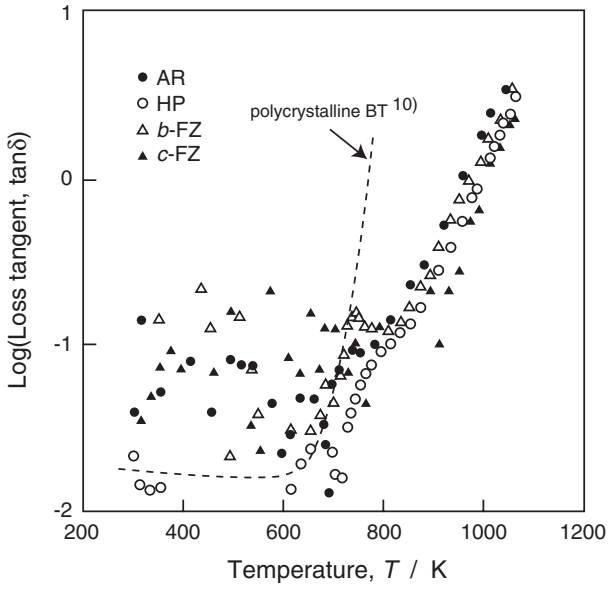

Fig. 8 Temperature dependence of loss tangent for poly- and single-crystalline BT_2 at 100 kHz.

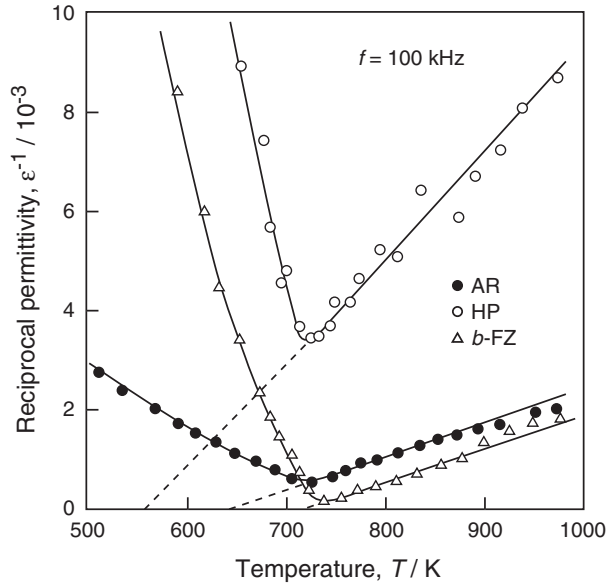

Fig. 7 Relationship between reciprocal permittivity and temperature for poly- and single-crystalline BT_2 at 100 kHz.

crystal defects such as oxide vacancy formed during the rapid quenching in Ar atmosphere. The high-temperature annealing in air may also affect the decrease of permittivity because the decomposition of BT_2 may locally proceed in grains. The HP specimen showed a peak ($\varepsilon = 300$) around 720 K resulting from the slight *b*-orientation as shown in Fig. 2(a). A small peak ($\varepsilon = 50$) was observed at 750 K for the *c*-FZ specimen. This may be caused of slight imperfection of *c*-orientation or small ferroelectricity in the *c*-direction.

Figure 7 demonstrates the relationship between the reciprocal permittivity (ε^{-1}) and temperature. It is generally known that the ε^{-1} commonly changes with temperature in many ferroelectric materials as given by eq. (1) over the Curie temperature (T_c).[15)]

$$\varepsilon^{-1} = C^{-1} \cdot (T - T_0) \quad (1)$$

where C is a constant, and T_0 is called as Curie-Weiss temperature. The T_0 values of AR, HP and *b*-FZ specimens were 642, 554 and 718 K, respectively. The C values were 1.52×10^5, 4.86×10^4 and 1.53×10^5 K, respectively. Akishige *et al.* have reported that the T_0 and C of single-crystalline BT_2 prepared by a flux method was 692 K and 3×10^5 K, respectively.[8)] These values were close to those of *b*-FZ specimens. Although the transition behavior around T_c for BT_2 has been scarcely reported, BT has been widely investigated due to its wide applications. Abdelkefi *et al.* reported that the T_0 and T_c of poly-crystalline BT was 365 and 395 K, respectively.[16)] The difference between T_c and T_0 of poly-crystalline BT was about 30 K. Drougard *et al.* reported that the T_0 and T_c of single-crystalline BT was 385 and 395 K, respectively.[17)] It is commonly understood that the T_0 is always lower than T_c, typically 10 K for reliable specimens of BT, which suggests the first order transition.[18)] In the present study, the difference of T_c and T_0 for BT_2 specimens ranged from 15 to 169 K. The smallest difference for BT_2 was almost the same as that of BT. The phase transition mechanism of BT_2 has been studied by Yashima *et al.*, and reported as $C2$ to $C2/m$ transition likely to be the first order transition.[19)]

Figure 8 shows the temperature dependence of dielectric loss ($\tan\delta$) for all specimens at 100 kHz. The $\tan\delta$ slightly decreased or almost constant with increasing temperature up to around the T_c, and then increased significantly. The $\tan\delta$ of AR specimen was highest among the all specimens. This suggests that the AR specimen has more defects sensitive to the ac field than the *b*-FZ specimen. The significant increase in the $\tan\delta$ over T_c could be contributed from the DC loss.[20)] In Fig. 8, the $\tan\delta$ of BT was compared with that of BT_2. The BT had low $\tan\delta$ values (smaller than 0.02) in a temperature range of 300 to 500 K; however, it increased significantly with increasing temperature above 600 K.[10)]

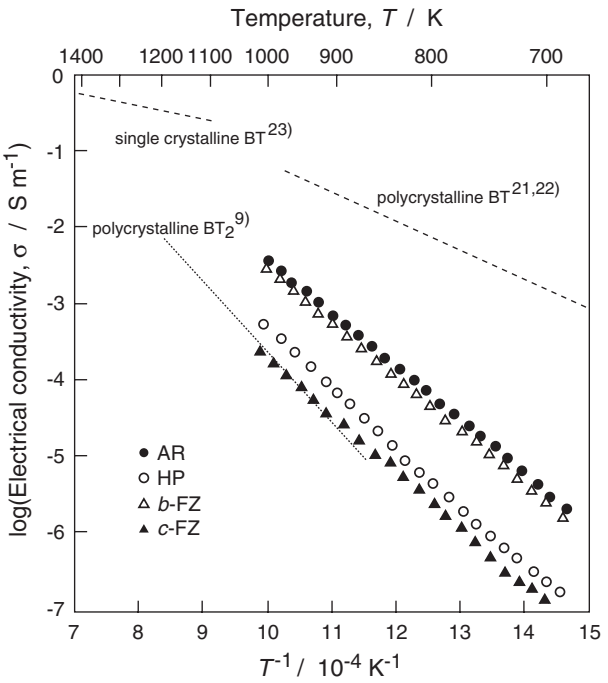

Fig. 9 Temperature dependence of electrical conductivity of poly- and single-crystalline BT_2.

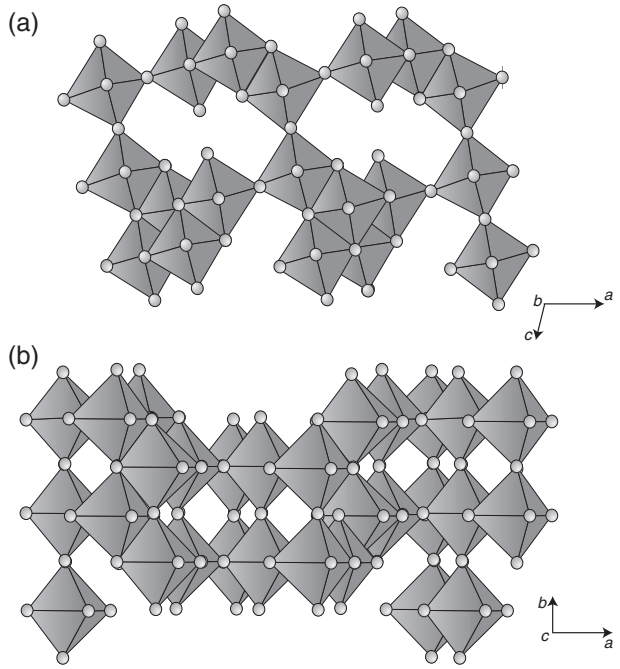

Fig. 10 Configuration of TiO_6 octahedrons in (a) *ac* and (b) *ab* planes.

Therefore, the BT_2 could be advantageous for applications due to its high ε and low $\tan\delta$ at high-temperatures around 600 to 900 K.

Figure 9 shows the temperature dependence of electrical conductivity (σ) of the BT_2 specimens comparing with poly- and single-crystalline BT. The electrical conductivities of AR and *b*-FZ specimens were almost the same, and about 10 times as high as that of *c*-FZ specimens. The σ of *b*-FZ and AR was 2 orders lower than that of poly-[21,22] and single-crystalline BT.[23] The HP specimen had intermediate values between *b*-FZ and *c*-FZ specimens. The crystal structure of BT_2 can be drawn by the combination of corner- and edge-shared TiO_6 octahedrons.[24] The arrangement of TiO_6 octahedrons is highly anisotropic. The connection of TiO_6 octahedrons is rather staggered in the *a*- and *c*-directions, and is well ordered in the *b*-direction as depicted in Figs. 10 (a) and (b), respectively. The ordering of TiO_6 octahedrons might associated with the anisotropy of the electrical conductivity of BT_2. The difference of σ between poly- and single-crystalline for BT_2 was greater than that for BT. This could be caused of the greater crystallographic anisotropy of BT_2 than that of BT.

4. Conclusions

Non-oriented and (010) oriented poly-crystalline BT_2 were prepared by hot-pressing and arc-melting, respectively. The maximum permittivity of non-oriented and (010) oriented poly-crystalline BT_2 was 300 and 2000 at 720 K, respectively, whereas that of BT_2 single-crystalline parallel to (010) and (001) was 6000 and 50 at the T_c (750 K). The $\tan\delta$ of all specimens were between 0.01 and 0.2 below T_c and significantly increased with increasing temperature above T_c. The electrical conductivity of (010) oriented poly- and single-crystalline BT_2 had almost same values, which were one order higher than that of non-oriented poly-crystalline BT_2 and (001) oriented single-crystalline BT_2.

Acknowledgements

The study was supported partly by the Grant-in-Aids for Exploratory Research (17656209) and the Scientific Research of Priority Areas (440-17042008) of the Ministry of Education, Culture, Sports, Science and Technology (MEXT), and the Asian CORE Program of the Japan Society for the Promotion of Science (JSPS).

REFERENCES

1) H. M. O 'Bryan, Jr. and J. Thomson, Jr.: J. Am. Ceram. Soc. **57** (1974) 522–526.
2) D. E. Rase and R. Roy: J. Am. Ceram. Soc. **38** (1955) 102–113.
3) T. Negas, R. S. Roth, H. S. Parker and D. Minor: J. Solid State Chem. **9** (1974) 297–307.
4) J. J. Ritter, R. S. Roth and J. E. Blendell: J. Am. Ceram. Soc. **69** (1986) 155–162.
5) K. W. Kirby and B. A. Wechsler: J. Am. Ceram. Soc. **74** (1991) 1841–1847.
6) T. Akashi, H. Iwata and T. Goto: Mater. Trans. **44** (2003) 1644–1646.
7) T. Akashi, H. Iwata and T. Goto: Mater. Trans. **44** (2003) 802–804.
8) Y. Akishige, K. Fukano and H. Shigematsu: Jpn. J. Appl. Phys. **42** (2003) L946–L948.
9) H. Beltrán, B. Gómez, N. Masó, E. Cordoncillo, P. Escribano and A. R. West: J. Appl. Phys. **97** (2005) 084104.
10) Y. Akishige and H. Shigematsu: J. Korean Phys. Soc. **46** (2005) 24–28.
11) J. T. S. Irvine, D. C. Sinclair and A. R. West: Adv. Mater. **2** (1990) 132–138.
12) A. R. West, D. C. Sinclair and N. Hirose: J. Electroceramics **1** (1997) 65–71.
13) W. Preis, A. Burgermeister, W. Sitte and P. Supancic: Solid State

Ionics **173** (2004) 69–75.
14) D. C. Sinclair and A. R. West: J. Appl. Phys. **66** (1989) 3850–3856.
15) C. Kittel: *Introduction to Solid State Physics*, pp. 467–483.
16) H. Abdelkefi, H. Khemakhem, G. Vélu, J. C. Carru and R. Von der Mühll: J. Alloys Compounds **399** (2005) 1–6.
17) M. E. Drougard and D. R. Young: Phys. Rev. **95** (1954) 1152–1153.
18) D. Richter and S. Trolier-McKinstry: *Nanoelectronics and Information Technology*, (Wiley-VCH, Weinheim, 2003) p. 59.
19) M. Yashima, R. Tu, T. Goto and H. Yamane: Appl. Phys. Lett. **87** (2005) 101909.
20) Y. Wu, M. J. Forbess, S. Seraji, S. J. Limmer, T. P. Chou and G. Cao: J. Appl. Phys. **89** (2001) 5647–5652.
21) T. Akashi, K. Morita, T. Hirai, H. Yamane and T. Goto: Mater. Trans. **42** (2001) 1823–1826.
22) N. Hirose and A. R. West: J. Am. Ceram. Soc. **79** (1996) 1633–1641.
23) J. Nowotny and M. Rekas: Ceramics International **20** (1994) 225–235.
24) T. Kimura, T. Goto, H. Yamane, H. Iwata, T. Kajiwara and T. Akashi: Acta Cryst. C **59** (2003) i128–130.